

# Raman and Optical Studies of spray pyrolysed $\text{Sb}_2\text{S}_3$ thin films

M. MEDLES<sup>a</sup>, N. BENRAMDANE<sup>a</sup>, A. BOUZIDI<sup>a</sup>, K. SAHRAOUI<sup>a</sup>, R. MILOUA<sup>a</sup>, R. DESFEUX<sup>b</sup>, C. MATHIEU<sup>b</sup>

<sup>a</sup>Laboratoire d'Elaboration et de Caractérisation des Matériaux, Université Djillali Liabes, Sidi Bel Abbes, Algeria

<sup>b</sup>Université d'Artois, Faculté Jean Perrin, Rue Jean Souvraz, SP18, 62307, Lens, France

Thin films of  $\text{Sb}_2\text{S}_3$  have been prepared by spray pyrolysis technique. Thiourea ( $\text{CS}(\text{NH}_2)_2$ ) and Antimony Trichloride ( $\text{SbCl}_3$ ) have been used as starting chemicals for the thin films preparation. The film surface morphology has been analyzed using the AFM (Atomic Force Microscope) and revealed that crystallites of average size of 620 nm compose the films of  $\text{Sb}_2\text{S}_3$ . Raman vibration mode assignments confirmed the identification of the  $\text{Sb}_2\text{S}_3$  phase for the prepared thin films and revealed that their Raman spectra are roughly dominated by stretching vibration modes  $\nu(\text{Sb-S})$ . The optical constants analysis of the prepared films gave 1.78 eV as a value of the optical band gap and confirmed the ionic character of the  $\text{Sb}_2\text{S}_3$  material.

Received March 01, 2014; accepted May 15, 2014)

**Keywords:**  $\text{Sb}_2\text{S}_3$ , X-ray diffraction, Raman spectroscopy, Spray Pyrolysis.

## 1. Introduction

Group V-VI compound thin films have potential applications in optoelectronic and photoelectrochemical devices, thermoelectric coolers, solar selective and decorative coatings. A numerous of methods have been employed for the preparation of group V-VI compound thin films. Stibnite ( $\text{Sb}_2\text{S}_3$ ) belongs to this class of materials, it is a layer-structured semiconductor with orthorhombic crystal structure [1]. Antimony trisulphide finds some special applications in the target materials for television cameras, microwave, switching and various optoelectronic devices [2-6].

Various methods have been employed to prepare  $\text{Sb}_2\text{S}_3$  thin and thick films. Savadogo and Mondal [7] have obtained amorphous  $\text{Sb}_2\text{S}_3$  thin films from aqueous chemical bath and reported a bandgap energy of 1.8 eV. Desai and Lokhande [8] have chemically deposited amorphous  $\text{Sb}_2\text{S}_3$  thin films using thioacetamide and tartaric acid as the  $\text{S}^{2-}$  ion source and complexing agent, respectively, and reported bandgap energy of 1.62 eV. Pawar *et al.* [9] have prepared  $\text{Sb}_2\text{S}_3$  thin films using a gas-solution interface technique. Vesguade *et al.* [10] have electrodeposited polycrystalline  $\text{Sb}_2\text{S}_3$  thin films from aqueous medium. Bhosale *et al.* [11] have prepared amorphous  $\text{Sb}_2\text{S}_3$  thin films by spray pyrolysis method with a band gap of 1.55 eV using oxalic acid as a complexing agent. Mane *et al.* [12] have deposited  $\text{Sb}_2\text{S}_3$  thin films from non-aqueous medium by chemical bath deposition. Killedar *et al.* [13] have prepared polycrystalline  $\text{Sb}_2\text{S}_3$  thin films from non-aqueous medium using  $\text{SbCl}_3$  and thiourea as  $\text{Sb}^{3+}$  and  $\text{S}^{2-}$  ions, respectively, using spray pyrolysis technique. Among all these techniques, the latter one is particularly attractive because of its simplicity [14]. It is widely used for large scale production of films owing to low production cost. It

is also fast, inexpensive, vacuum-less and suitable for mass production. All these factors make so that one chose this technique for the preparation of our films of  $\text{Sb}_2\text{S}_3$ .

According to our bibliographical study, no report was given on detailed Raman assignment on spray pyrolysed thin films of  $\text{Sb}_2\text{S}_3$ .

The present work is focused on the Raman vibrational mode assignments and the optical dispersion study of spray pyrolysed thin films of  $\text{Sb}_2\text{S}_3$ . The phase identification of  $\text{Sb}_2\text{S}_3$  thin films and structural characterization were performed by x-ray diffraction (XRD). The optical dispersion study based on the optical constant spectra has been performed using an adapted computing method for the optical constants determination and avoiding the errors of the optical measurements of the reflectances and transmittances caused by the effect of the substrates on which our films of  $\text{Sb}_2\text{S}_3$  were deposited.

## 2. Experimental

The thin films of  $\text{Sb}_2\text{S}_3$  were deposited by spray pyrolysis technique on amorphous glass substrates with dimensions of  $75 \times 25 \text{ mm}^2$  for 10 seconds, with 2 minutes interval between spraying periods in order to avoid excessive cooling of the glass substrates resulting from continuous spray. The deposition process starts by cleaning the glass substrates in diluted chlorhydric acid (HCl), washed by double distilled water and dried. The used spraying solutions have been obtained by dissolving the antimony trichloride  $\text{SbCl}_3$  (purity: 99.98%) and thiourea  $\text{CS}(\text{NH}_2)_2$  (purity: 99.98%) in doubly distilled water with a concentration of 0.2 M. In 20 ml of (0.2 M)  $\text{SbCl}_3$  solution 2.5 ml of chlorhydric acid (1 M) solution was added. The prepared clear solutions of antimony trichloride and thiourea have been appropriately mixed to

obtain a Sb:S proportion of 2:3. Compressed air at a pressure of  $6 \times 10^4$  Pa has been used as a carrier gas. In this preparation process, the following conditions have been used: substrate temperature 470 K, solution flow of 5 cm<sup>3</sup>/min, spray nozzle to heating plaque distance of 27 cm. One also notes that the prepared solutions were immediately sprayed to avoid any possible chemical changes with time.

Structural characterization has been carried out at room temperature using a Phillips 1830 powder diffractometer working at CuK<sub>α</sub> peak with wavelength  $\lambda = 0.15406$  nm. AFM measurements have been performed in air using a Park Scientific Instrument. Autoprobe CP Scanning Force Microscope that operates with an optical deflection sensor force. The imaging has been performed with microfabricated Si<sub>3</sub>N<sub>4</sub> cantilevers and microlever tips using a small repulsive force.

Raman spectroscopy measurements have been performed at room temperature in a backscattering microconfiguration using the 514.5 nm line from an Ar-ion laser focused on the surface as a spot of 1 μm in diameter and with a power density of  $\sim 3$  mW/cm<sup>2</sup>. The scattered light has been analyzed with a Jobin Yvon T64000 spectrometer, equipped with a liquid nitrogen cooled CCD detector. The spectrometer provided a wave number resolution better than 3 cm<sup>-1</sup>.

The optical transmittances and reflectances have been recorded from 300 to 1800 nm wavelength using a UV(ultra-violet)/visible JASCO type V-570 double beam spectrophotometer (resolution: 0.1 nm).

### 3. Results and discussion

Fig.1 shows a diffraction spectrum of Sb<sub>2</sub>S<sub>3</sub> thin films deposited on glass-substrate according to the experimental conditions mentioned previously. The measured spectra present well-defined peaks which are in good agreement with the peak positions of standard Sb<sub>2</sub>S<sub>3</sub> : Stibnite, JCPDS (Joint Committee of Powder Diffraction Standards) N° 42-1393.

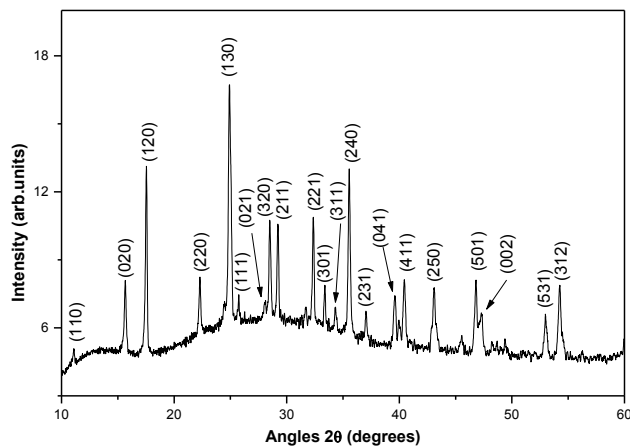
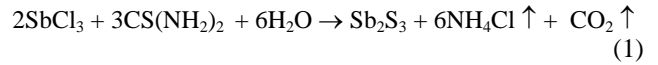


Fig. 1. X-ray diffraction patterns of Sb<sub>2</sub>S<sub>3</sub> thin films prepared by spray pyrolysis method.

For films of Sb<sub>2</sub>S<sub>3</sub> formed by pyrolysis reaction on the glass-substrate surface of the solution pulverized particles, the following thermochemical reaction is suggested:



In order to determine the orthorhombic lattice parameters, we have used the quadratic relation:

$$d_{hkl} = \frac{1}{\sqrt{\frac{h^2}{a^2} + \frac{k^2}{b^2} + \frac{l^2}{c^2}}} \quad (2)$$

where  $(h, k, l)$  are Miller indices of reflecting planes appearing on the diffraction spectrum and  $d_{hkl}$  their inter-reticular distances. The obtained values of structural parameters  $a$ ,  $b$ , and  $c$  are 11.1193 nm, 1.1306 nm and 0.3844 nm respectively and are in good agreement with those already given [15-17].

The AFM image of spray pyrolysed films of Sb<sub>2</sub>S<sub>3</sub> is shown in the Fig. 2. The morphology shows small sheets laid out in more or less regular configurations. According to our bibliographical study, these features were never observed for the thin films of Sb<sub>2</sub>S<sub>3</sub>.

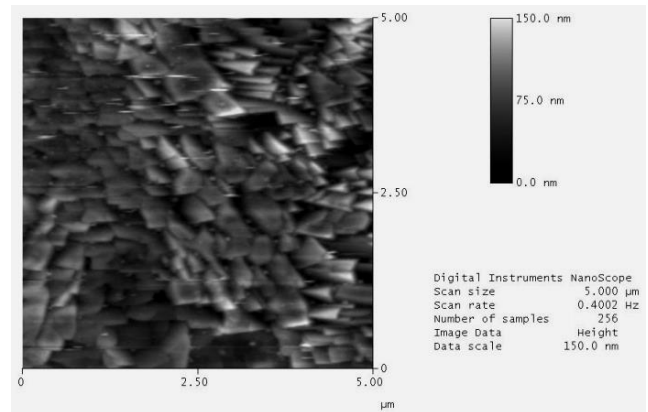


Fig. 2. AFM image of the surface morphology of spray pyrolysed Sb<sub>2</sub>S<sub>3</sub> thin films.

By direct observation using Fig. 2, the image revealed that the crystallites, shaped in sheets, of average size around 620 nm, compose the spray pyrolysed films of Sb<sub>2</sub>S<sub>3</sub>.

The degree of preferred orientation  $P_{hkl}$  was calculated from the peaks intensities of wide angle scan using the method of Harris [18] for polycrystalline fibre texture analysis:

$$P_{hkl} = N \left( \frac{I_{hkl}}{I_{hkl}^0} \right) \left( \sum_{hkl=1}^N \frac{I_{hkl}}{I_{hkl}^0} \right)^{-1} \quad (3)$$

where  $N$  is the number of peaks in the angular range considered,  $I_{hkl}$  is the measured intensity of peak  $(hkl)$ , and  $I_{hkl}^0$  is the relative intensity of the corresponding peak from a random powder standard. For  $P_{hkl}=N$ , all the crystallites of the films are oriented in the  $\langle hkl \rangle$  direction normal to the specimen plane, while  $P_{hkl}=1$  indicates random crystallite orientations and  $P_{hkl}<1$  indicates a preferred orientation along an axis other than  $\langle hkl \rangle$ . In our case, computed values of  $P_{hkl}$  for the most intense peaks

corresponding to planes (130) and (120) gave  $P_{130} \cong 1$  and  $P_{120} \cong 1$  which indicates a random crystallite orientations.

The Raman spectrum of the investigated  $Sb_2S_3$  films obtained by the spray pyrolysis technique was measured at room temperature and presented in Fig. 3.a. The spectrum exhibit broad band between 200 and 400  $cm^{-1}$  which is considered the characteristic spectral region of sulfide [19,20]. The comparison of our spectrum, Fig. 3.a with the spectrum obtained from the RUFF database (Fig. 3.b [21]), shows similarities in the overall main peak positions.

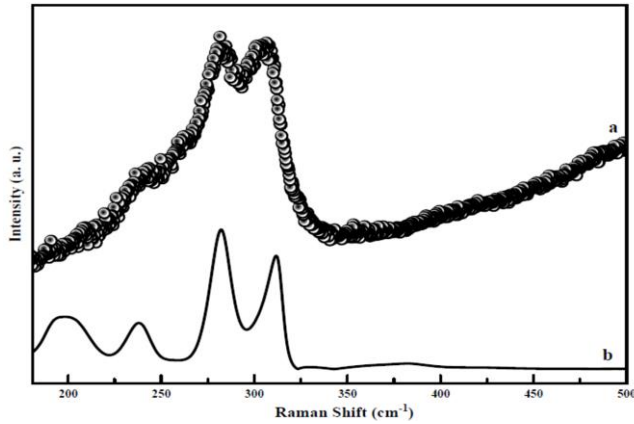


**Fig. 3.** Raman spectra of  $Sb_2S_3$  thin films obtained; **a)** our measured spectrum of  $Sb_2S_3$  thin films obtained; **b)** spectrum of unoriented sample of  $Sb_2S_3$ , obtained from the RRUFF data-base, RRF ID: R050066.2 [21].

In order to analyze our experimental spectrum, we have performed spectral decompositions of the Raman broad-bands as shows in Fig. 4. The experimentally measured broad-bands result from the convolution of the Lorentzian profile of the Raman modes.

The spectral decomposition reveals (Fig. 4) the presence of seven bands at 190, 207, 238, 251, 282, 302 and 310  $cm^{-1}$ .

It is well known that Stibnite  $Sb_2S_3$  is isostructural [22-25] and crystallizes in orthorhombic crystal lattice structure. According to the structural results [22,23], the corresponding space group is  $Pnma$  ( $D_{2h}^{16}$ ).

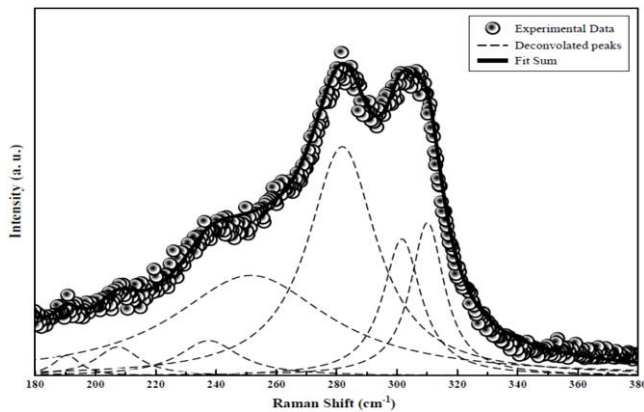


**Fig. 4.** Decomposition of the Raman spectrum of  $Sb_2S_3$  thin films obtained.

The crystal structure of  $Sb_2S_3$  is formed of 1-D ribbons of polymerized  $(Sb_4S_6)_n$  and each ribbon is linked to its four neighbors by weak Sb-S and S-S bonds [22]. It was suggested that the basic structural units in  $Sb_2S_3$  are  $SbS_3$  pyramids ( $C_{3v}$ ) [22]. According to Nakamoto [26], an isolated ideal pyramidal  $SbS_3$  groups show only four normal modes of vibration ( $2A_1+2E$ ) which are both Raman and infrared active (Fig.5). The two stretching frequencies symmetric  $\nu_s(A_1)$  and antisymmetric  $\nu_a(E)$ , as well as the two bending frequencies, symmetric  $\delta_s(A_1)$  and antisymmetric  $\delta_a(E)$ , overlap or are close in energy in most similar compounds which show also  $\nu_s > \nu_a$  and  $\delta_s > \delta_a$  tend [26].

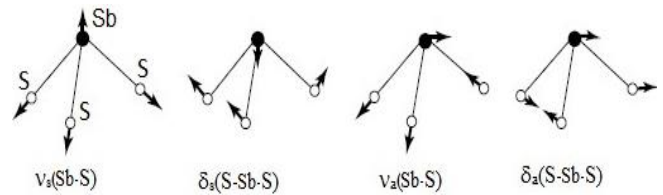


**Fig. 5** Normal modes of vibration of pyramidal  $SbS_3$  molecules[26].

According to the  $D_{2h}^{16}$  factor group ( $k=0$ ), the crystal modes can be classified as follows:

$$\Gamma_{opt} = 10A_g + 5B_{1g} + 10B_{2g} + 5B_{3g} + 5A_u + 10B_{1u} + 5B_{2u} + 10B_{3u} \quad (4)$$

all g modes are Raman-active and only,  $B_u$  modes are IR active and the  $A_u$  one is silent.

Correlating this with data from literature led us to assign the bands in Raman spectrum of  $Sb_2S_3$  ( Fig. 4 and Table 1). The tentative band assignments (Tab. 1) are based on the sequence of band energies given by Nakamoto [26] with  $\nu_s > \nu_a > \delta_s > \delta_a$  and facilitated by comparing the band positions with those given in the works of P. Sereni *et al.* [27] and S. Kharbish *et al.* [28].

The observed bands at 282 and 302  $cm^{-1}$  corresponded to antisymmetric stretching vibrations  $\nu_a(Sb-S)$ , whereas, the band at 310  $cm^{-1}$  was attributed to symmetric stretching vibrations  $\nu_s(Sb-S)$ . On the other hand, the bands at 251 and 238  $cm^{-1}$  corresponded to symmetric bending vibrations  $\delta_s(S-Sb-S)$ , when those at 190 and 207  $cm^{-1}$  were attributed to antisymmetric bending vibrations  $\delta_a(S-Sb-S)$ .

Table 1 shows the comparison of our frequency vibration values and their assignment with those given by other authors. We note that there is a good agreement between our results and those previously given for  $Sb_2S_3$  single crystal. On the other hand, Fig. 4 and Table 1 show that Raman spectra of spray pyrolysed  $Sb_2S_3$  thin films are roughly dominated by stretching vibrations at frequencies 282, 302 and 310  $cm^{-1}$ .

Table 1. Experimental frequencies (cm<sup>-1</sup>) and Raman assignment of active modes for Sb<sub>2</sub>S<sub>3</sub> thin films obtained.

	Symmetry	Band cm <sup>-1</sup>	Other works	
			Band cm <sup>-1</sup> [20]	Band cm <sup>-1</sup> [27]
v <sub>s</sub> (Sb-S)	B <sub>1g</sub>	306	310	310
v <sub>a</sub> (Sb-S)	B <sub>1g</sub>	300	300	303
	A <sub>g</sub>	282	281	283
δ <sub>s</sub> (S-Sb-S)	A <sub>g</sub>	251	254	256
	B <sub>1g</sub>	237	237	239
δ <sub>a</sub> (S-Sb-S)	B <sub>1g</sub>	207	207	207
	B <sub>1g</sub>	190	189	192

v<sub>s</sub>: symmetric stretching vibration; v<sub>a</sub>: antisymmetric stretching vibration; δ<sub>s</sub>: symmetric bending vibration; δ<sub>a</sub>: antisymmetric bending vibration.

The determination of the optical constants (n, k) was carried out by applying the method used in our previous paper [29]. In the present work, the system of three nonlinear equations was reduced to two nonlinear equations by imposing the thickness as a known parameter.

$$\begin{cases} A_1(n, k, d) - A_1(\lambda) = 0 \\ A_2(n, k, d) - A_2(\lambda) = 0 \\ A_3(n, k, d) - A_3(\lambda) = 0 \end{cases} \Rightarrow \begin{cases} A_1(n, k) - A_1(\lambda) = 0 \\ A_2(n, k) - A_2(\lambda) = 0 \end{cases} \quad (5)$$

The imposed thickness value was determined by AFM observation. Once all the spectrophotometric measurements necessary to perform the computing method are done on the test sample, a small scratch is created by removing mechanically the Sb<sub>2</sub>S<sub>3</sub> matter of the thin film deposited on the glass substrate (Fig. 6.a). The AFM observation by scanning the step edge allows the thickness measurement.

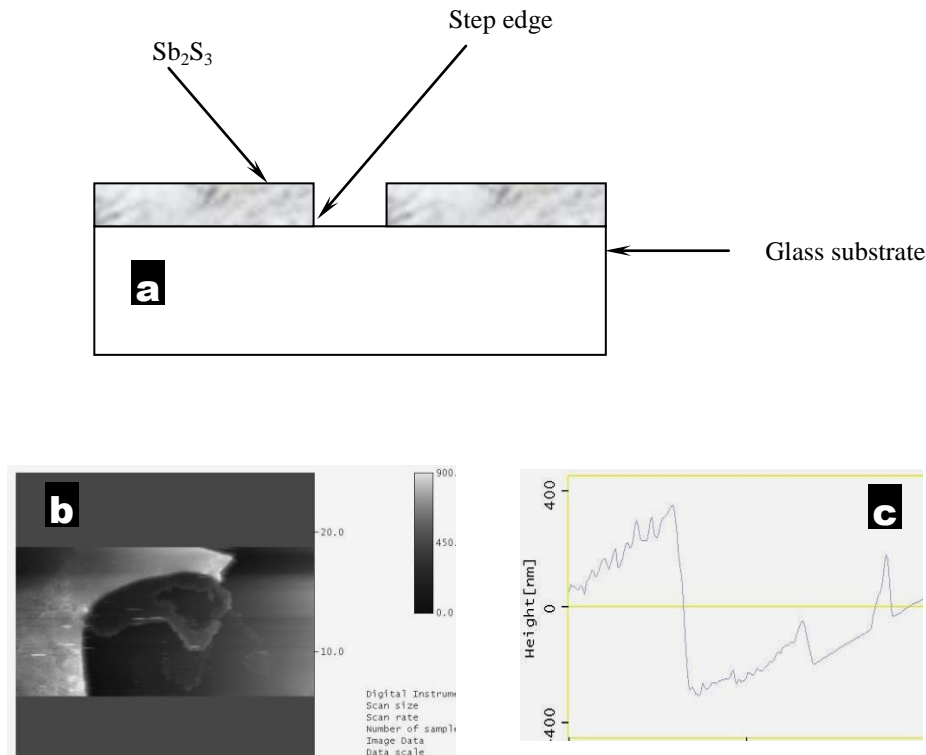


Fig. 6. Thickness determination of the test sample of Sb<sub>2</sub>S<sub>3</sub> thin film; a) Sb<sub>2</sub>S<sub>3</sub> test sample geometry used in the thickness measurement; b) AFM image to estimate the test sample thickness of Sb<sub>2</sub>S<sub>3</sub>; c) Profilograph of the step edge in the test sample of Sb<sub>2</sub>S<sub>3</sub> thin film.

The estimated value of test sample thickness (by direct observation) was 634 nm (Figs. 6. b and 6.c.). Fig. 7 shows the spectral behaviors of *n* and *k* obtained in the energy range (1–3.5 eV). The refractive index (*n*) of the thin films of Sb<sub>2</sub>S<sub>3</sub> prepared by spray pyrolysis method,

has a value of 3 at low energies and a value around 4.3 at high energies. It is characterized by a continuously growth with the energy increasing. Furthermore, the extinction index (*k*) has 0.37 as maximum value at about 2.4 eV.

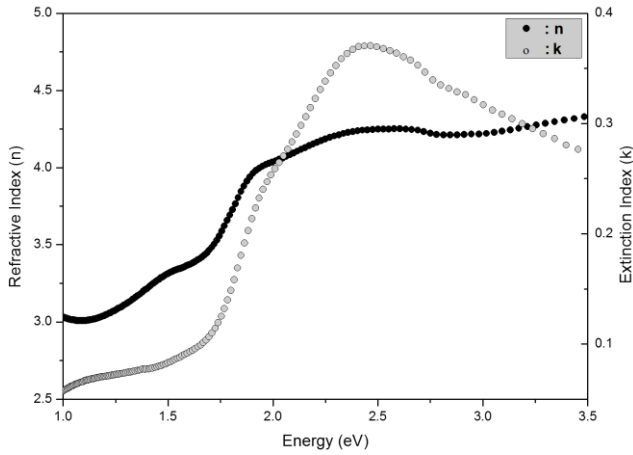


Fig. 7. Spectral behaviors of the refractive index ( $n$ ) and the extinction coefficient ( $k$ ) of spray pyrolysed  $Sb_2S_3$  thin films.

The absorption coefficient (Fig. 8) was calculated from the extinction index ( $\alpha = 4\pi k / \lambda$  [27]). In the absorption process, a photon of known energy excites an electron from a lower to a higher energy state, corresponding to an absorption edge. In noncrystalline materials (polycrystalline and amorphous materials) a typical absorption edge can be broadly ascribed to either of the three processes: (i) residual below-gap absorption, attributed to the light diffusion by the geometrical defects on film surface [30], (ii) Urbach tails, due to topological disorder [31] and (iii) interband absorption with a power law shape, due to fundamental transitions [32].

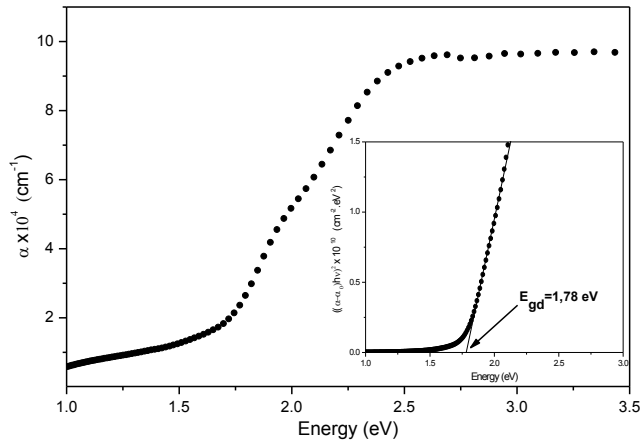


Fig. 8. Absorption spectrum of spray pyrolysed thin films of  $Sb_2S_3$ .

The absorption coefficient variation as a function of incident photon energy, according to the intrinsic electronic transitions theory, is given by [31]

$$(\alpha - \alpha_0)h\nu = A(h\nu - E_{gd})^{1/2} \quad (6)$$

$h\nu$  is the incident photon energy and  $E_{gd}$  is the optical gap for direct transitions,  $\alpha_0$  is the residual absorption and  $A$  is the practically constant parameter. The use of  $\alpha_0$  in

this relation allows in overcoming the error caused by the residual absorption, not existent in the perfect crystalline material.

The linear region extrapolation in  $((\alpha - \alpha_0)h\nu)^2$  energy dependence curve (Fig. 9) gives the optical gap energy of the allowed direct transitions for the  $Sb_2S_3$  thin films. From the intercept it is found that  $E_{gd} = 1.78$  eV. This value of the band gap is in the range of the values already given by various authors [7-8,11]. In the thin films field, often, the authors give different values for the band gap for the studied material. These different values of band gap could be explained by the effect of crystallite size on the optical band in polycrystalline thin films of semiconductor. This effect has been discussed by many researchers [31,33].

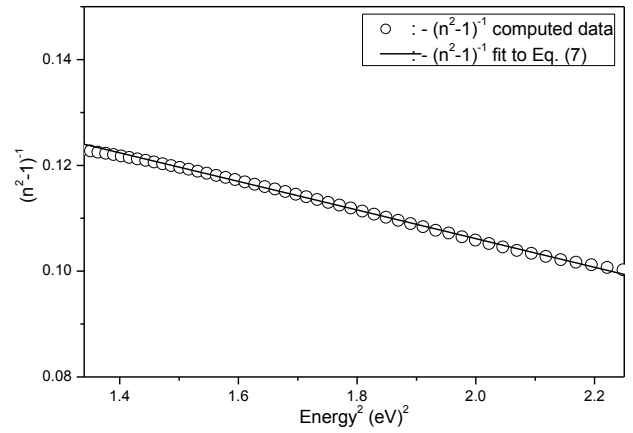


Fig. 9. Plot of  $(n^2 - 1)^{-1}$  versus  $E^2$  of spray pyrolysed  $Sb_2S_3$  thin films.

According to the dispersion theory in the region of low absorption, the refractive index ( $n$ ) is given in a single-oscillator model by the expression [34-37]:

$$n^2 - 1 = \frac{E_0 E_d}{E_0^2 - E^2} \quad (7)$$

where  $n$ , is the refractive index,  $E_0$  is the energy of the effective dispersion oscillator,  $E$  is the photon energy, and  $E_d$  is the so-called dispersion energy. The latter quantity measures the average length of interband optical transitions.

The straight line fitting to the points in the curve of  $(n^2 - 1)^{-1}$  against  $E^2$  allows the oscillator parameters determination. The values obtained of  $(E_0, E_d)$  are 2.69 eV and 16.85 eV respectively.

According to Takana [34] the relationship between the energy  $E_0$  and the gap, which is also derived from the Wemple-DiDominico [35-37] dispersion analysis, must have a value between 1.5 and 2. In our case, we found  $E_{gd} \approx E_0/1.5 \approx 1.78$  eV. This obtained optical gap energy value from single-oscillator model is in good agreement with that determined from the absorption coefficient according to the intrinsic electronic transitions theory.

On the other hand, it has been remarked by S. Wemple and DiDominico [35-37] for widely different

ionic and covalent crystalline solids that the dispersion energy  $E_d$  obeys the equality relationship:

$$\beta = \frac{E_d}{Z_a N_e N_c} \quad (8)$$

where  $\beta = 0.26 \pm 0.04$  [36] for the ionic materials and  $0.39 \pm 0.04$  [36] for the covalent ones,  $N_c$  is the coordination number of the cation nearest neighbor to the anion,  $Z_a$  is the formal chemical valency of the anion and  $N_e$  is the total number of valence electrons (cores excluded) per anion. In our case,  $Z_a=2$  for a Sulphur atom,  $N_c=3$  (basic structural units: SbS<sub>3</sub> pyramids [22]) and  $N_e=9.33$  which yields  $\beta = 0.30$  for Sb<sub>2</sub>S<sub>3</sub> thin films obtained. This value is in agreement with the ionic character of the Sb<sub>2</sub>S<sub>3</sub> material already mentioned in the work of H. Koc et al [38].

#### 4. Conclusion

Thin films of Sb<sub>2</sub>S<sub>3</sub> have been obtained by spray pyrolysed technique. The structural study showed that the films of Sb<sub>2</sub>S<sub>3</sub> obtained, exhibit random crystallite orientations. The surface morphology of the obtained films has been analysed using the AFM image. Crystallites of average size of 620 nm compose the prepared films of Sb<sub>2</sub>S<sub>3</sub>. The Raman spectroscopy confirmed the identification of the Sb<sub>2</sub>S<sub>3</sub> phase for the prepared thin films and showed that their Raman spectra are roughly dominated by stretching vibration modes  $\nu(\text{Sb-S})$  corresponding to frequencies at 282, 302 and 3010 cm<sup>-1</sup>. The dispersion analysis confirmed the ionic character of the Sb<sub>2</sub>S<sub>3</sub> material. The value of the optical band gap energy of the obtained thin films of Sb<sub>2</sub>S<sub>3</sub>, determined from single-oscillator model and from the intrinsic electronic transitions theory, has been estimated to 1.78 eV.

#### References

- [1] A. Kyono, M. Kimata, M. Matsuhisa, Y. Miyashita, K. Okamoto, *Phys. Chem. Minerals*, **29**, 254 (2002).
- [2] J. Grigas, J. Meshkanskas, A. Orliakas. *Phys. Stat. Sol. (a)* **37**, K39 (1976).
- [3] M. S. Ablowa, A. A. Andreev, T. T. Dedagkaev, B. T. Melekh, A. B. Penstsov, N. S. Sheridel, L.N. Shumilova. *Sov. Phys. Semicond.* **10**, 629 (1976).
- [4] J. George, M. K. Radhakrishnan, *Solid State Commun.* **33**, 987 (1980).
- [5] B. R. Sankapal, R. S. Mane, C. D. Lokhande, *Journal of Materials Science Letters* **18**, 1453 (1999).
- [6] R. S. Mane, C. D. Lokhande, *Materials Chemistry and physics* **78**, 385 (2002).
- [7] O. Savadogo, K. C. Mondal *J. Electrochem. Soc.* **141**, 2871 (1994).
- [8] J. D. Desai, C. D. Lokhande, *Thin Solid Films* **237**, 29 (1994).
- [9] S. H. Pawar, S.P. Tamhankar, P. N. Bhosale, M. D. Uplane, *Ind. J. Pure Appl. Phys.* **21**, 665 (1983).
- [10] N. S. Vesguade, C. D. Lokhande, C. H. Bhosale, *Thin Solid Films* **263**, 145 (1995).
- [11] C. H. Bhosale, M. D. Uplane, P. S. Patil, C. D. Lokhande, *Thin Solid Films* **248**, 137 (1994).
- [12] R. S. Mane, B. R. Sankapal, C. D. Lokhande, *Thin Solid Films* **353**, 29 (1999).
- [13] V. V. Killedar, C. D. Lokhande, C. H. Bhosale, *Mater. Chem. Phys.* **47**, 104 (1997).
- [14] Z. Kebbab, N. Benramdane, M. Medles, A. Bouzidi, H. Tabet-Derraz, *Sol. Energy Mater. Sol. Cells* **71**, 449 (2002).
- [15] K. Y. Rajpure, C. H. Bhosale, *Materials Chemistry and Physics* **73**, 6 (2002).
- [16] H. Hu, Z. Liu, B. yang, M. Mo, Q. Li, W. Yu, Y. Qian, *J. Crys. Growth* **262**, 375 (2004).
- [17] R. W. G. Wyckoff, *Crystal structures*, Wiley, New York, **2**, (1964).
- [18] K. Durose, S. E. Asher, W. Jaegermann, D. Levi, B. E. McCandless, W. Metzger, H. Moutinho, P. D. Paulson, *Prog. Photovoltaic: Res. Appl.* **12**, 177 (2004).
- [19] A. Wang, J. Han, L. Guo, J. Yu, P. Zeng, *App. Spectroscopy* **48**, 959 (1994).
- [20] S. Kharbish, *American mineralogist* **96**, 609 (2011).
- [21] <http://rruff.info>
- [22] J. Petzelt, J. Grigas, *Ferroelectrics* **5**, 59 (1973).
- [23] W. Hofmann, *Z. Kristallogr.* **86**, 225 (1933).
- [24] S. Sdavnizar, *Z. Kristallogr.* **114**, 85 (1960).
- [25] E. Dönges, *Z. Anorg. Chem.* **263**, 289 (1950).
- [26] K. Nakamoto, *Infrared and Raman Spectra of Inorganic and Coordination compounds*, Fourth Editions, John Wiley & Sons, São Paulo, 1986.
- [27] P. Sereni, M. Musso, P. Knoll, P. Blaha, K. Schwarz, G. Schmidt, *AIP Conf. Proc.* **1267**, 1131 (2010).
- [28] S. Kharbish, E. Libowitzky and A. Beran, *Eur. J. Mineral.* **21**, 325 (2009).
- [29] M. Medles, N. Benramdane, A. Bouzidi, A. Nakrela, H. Tabet-Derraz, Z. Kebbab, C. Mathieu, B. Khelifa, R. Desfeux, *Thin Solid Films*, **497**, 58 (2006).
- [30] J. Szczyrbowski, A. Czapca, *Thin Solid Films*, **46**, 127 (1977).
- [31] F. Urbach. *Phys. Rev.*, **92**, 1324 (1953).
- [32] P. Kireev, *La Physique des Semiconducteurs*, Mir, Moscow (1975).
- [33] M. Moskovits In: G. Soles, Editor, *Chemical Physics of Atomic and Molecular Clusters*, North Holland, Amsterdam, 1990.
- [34] K. Takana, *Thin Solid Film*, **66**, 271 (1980).
- [35] S.H. Wemple, M. DiDomenico, *Phys. Rev.*, **B 3**, 1338 (1971).
- [36] S. H. Wemple and M. DiDomenico, *Phys. Rev. Lett.*, **23**, 1156 (1969).
- [37] S.H. Wemple, M. DiDomenico, *Phys. Rev.*, **B 7**, 3767 (1973).
- [38] H. Koc, Amirullah M. Mamedov, E. Deligoz, H. Ozisik, *Physica B, Phys. of Cond. Mat.*, **406**, 287 (2011).

Corresponding author: m\_medles@yahoo.